Contents lists available at ScienceDirect

Chinese Chemical Letters

journal homepage: www.elsevier.com/locate/cclet

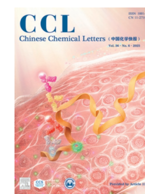

Enhanced durability of a novel thiol-epoxy network thermosets with excellent hygrothermal and chemical resistance

Chunshi He[a], Linqing Li[a], Yuanrong Sun[a], Xuefang Wang[b], Jie Ren[a], Jianbo Li[a,*]

[a] Innovation Center of Functional Adhesion and Coating Technology, Department of Polymeric Materials, School of Materials Science and Engineering, Tongji University, Shanghai 201804, China
[b] Industrial Research Institute of Nonwovens & Technical Textiles, College of Textiles & Clothing, Qingdao University, Qingdao 266071, China

ARTICLE INFO

Article history:
Received 30 November 2024
Revised 24 January 2025
Accepted 27 January 2025
Available online 27 January 2025

Keywords:
Thiol/epoxy thermosetting polymer
Low-temperature curing
Heat resistance
Chemical resistance
Hygrothermal resistance

ABSTRACT

Epoxy resin is widely used in electronic packaging due to its exceptional performance, particularly the low-temperature curable thiol/epoxy system, which effectively minimizes thermal damage to sensitive electronic components. However, the majority of commercial thiol curing agents contain hydrolysable ester bonds and lack rigid structures, which induces most of thiol/epoxy systems still suffering from unsatisfactory heat resistance and hygrothermal resistance, significantly hindering their application in electronic packaging. In this study, we synthesized a tetrafunctional thiol compound, bis[3-(3-sulfanylpropyl)-4-(3-sulfanylpropoxy)phenyl]sulfone (TMBPS) with rigid and ester-free structures to replace traditional commercial thiol curing agents, pentaerythritol tetra(3-mercaptopropionate) (PETMP). Compared to the PETMP/epoxy system, the TMBPS/epoxy system exhibited superior comprehensive properties. The rigid structures of bisphenol S-type tetrathiol enhanced the heat resistance and mechanical properties of TMBPS/epoxy resin cured products, outperforming those of PETMP/epoxy resin cured products. Notably, the glass transition temperature of TMBPS/epoxy resin cured products was 74.2 °C which was 11.8 °C higher than that of PETMP cured products. Moreover, the ester-free structure in TMBPS contributed to its enhanced resistance to chemicals and hygrothermal conditions. After undergoing 1000 h of high-temperature and high-humidity aging, the tensile strength and adhesion strength of TMBPS-cured products were 73.33 MPa and 3.39 MPa, respectively exceeding 100% and 40% of their initial values, while PETMP-cured products exhibited a complete loss of both tensile strength and adhesion strength. This study provides a strategy for obtaining thermosetting polymers that can be cured at low temperatures and exhibit excellent comprehensive properties.

© 2025 Published by Elsevier B.V. on behalf of Chinese Chemical Society and Institute of Materia Medica, Chinese Academy of Medical Sciences.

With the rapid development of modern industry, the requirements for material properties are increasing, especially the application requirements under extreme environmental conditions. Epoxy resin is a high-performance synthetic material, renowned for its excellent adhesion, mechanical properties, electrical insulation, as well as chemical and thermal stabilities [1–8]. Consequently, it is widely used across various industries, including construction [9], automotive [10], electronics [11] and aerospace [12]. Typically, epoxy resin presents liquid or semi-solid states at room temperature and requires curing to transform into a solid state. Common curing agents include amines [13–16], imidazoles [17], anhydrides [18,19], polyamides [20], and polythiols [21]. Most of these agents necessitate curing at elevated temperatures (approximately 120 °C or higher), inevitably resulting in some thermal damages to the resultant products. Thiol/epoxy systems that curing at a low temperature have garnered significant interest because of their benefits in energy conservation, enhanced production efficiency, and suitability for unique environments.

Over the past few decades, the researches focused on thiol curing agents have made some significant progresses. Alvaro *et al.* [22], added trifunctional thiol (trimethylolpropane tris(3-mercaptopropionate)) to epoxy resin and amino-terminated poly(hydroxyl polyurethane) system to accelerate the curing process, which proved that thiol curing agent had high activity. At the same time, some researchers began to study the factors affecting the activity of thiol curing agent. Hong *et al.* [23], explored the effect of molecular weight on the curing activity of curing agent by synthesizing two different molecular weight 2–hydroxy-3-mercaptopropyl terminated polypropylene glyceryl ether curing agents (HMP-t-PGE). Compared with high molecular weight HMP-t-PGE, low molecular weight HMP-t-PGE was more reactive, and

* Corresponding author.
E-mail address: lijianbo@tongji.edu.cn (J. Li).

https://doi.org/10.1016/j.cclet.2025.110905
1001-8417/© 2025 Published by Elsevier B.V. on behalf of Chinese Chemical Society and Institute of Materia Medica, Chinese Academy of Medical Sciences.

the gelation time of curing epoxy resin was about half of that of high molecular weight curing agent. Kim *et al.* [24], studied the effect of hydroxyl and methyl on the activity of thiol curing agent. They synthesized thiol-functionalized polysilsesquioxane containing hydroxyl and methyl groups by acid-catalyzed sol-gel method. Compared with the thiol curing agent containing methyl group, the thiol curing agent containing hydroxyl group showed higher reactivity, higher conversion rate and shorter curing time. Besides, other studies had shown that increasing the degree of functionality of the thiol curing agent can significantly increase the heat resistance and mechanical properties of the epoxy resin after thiol curing. Wang *et al.* [25], reacted trifunctional thiol, trimethylolpropane tris(3-mercaptopropionate) (TMP) and tetrafunctional thiol, pentaerythritol tetra(3-mercaptopropionate) (PMP) respectively with epoxy resin. The glass transition temperature and tensile strength of the tetrafunctional thiol cured product were about 20 °C and 20 MPa higher than those of the trifunctional thiol cured product, which demonstrated the effect of the degree of functionality on material properties. Lu *et al.* [26], prepared different numbers of thiol-terminated hyperbranched polymers (THBP-n, $n = 3, 6, 9, 12$) and used them to cure epoxy resin. With the increase of the degree of functionality, the heat resistance and mechanical properties of the cured epoxy resin showed an upward trend.

However, the current use of alkylated thiols leads to insufficient rigidity, which limits the heat resistance and mechanical properties of materials. To solve this problem, the introduction of benzene ring strategy [27,28] has also been developed. For example, Ke *et al.* [29], introduced the benzene ring into the difunctional thiol curing agent (BDB) and reacted it with the multi-arm epoxy resin (EHCPP). Compared with EHCPP cured by other aliphatic thiols, EHCPP cured by BDB showed the highest mechanical properties (tensile strength of 34.9 MPa) and thermal stability (carbon residue rate of 19.43%), indicating that the introduction of benzene ring into thiol molecules is an effective method. In addition, most thiol curing agents contain ester bonds, which makes the cured epoxy resin exhibit poor chemical stability and poor hygrothermal resistance, significantly weakening material performances. Therefore, it is very important to prepare a kind of thiol curing agent without ester bonds [30–32].

Herein, bis[3-(3-sulfanylpropyl)-4-(3-sulfanylpropoxy)phenyl] sulfone (TMBPS) was synthesized from bisphenol S in this study. This compound has unique structures, including two benzene rings, a polar sulphone group, four thiol groups and ester-free structure. TMBPS is based on a bisphenol backbone structure which provides good compatibility with general epoxy resins. Thiol/epoxy thermosetting polymers were prepared by reacting TMBPS with bisphenol a diglycidyl ether (DGEBA) (Scheme 1), using commercial thiol pentaerythritol tetra(3-mercaptopropionate) (PETMP) as a control. A thorough investigation was conducted on various aspects of the thiol/epoxy thermosetting polymers, including curing behavior, rheological properties, heat resistance, chemical resistance, water resistance, mechanical properties, UV-shielding properties and dielectric properties. In addition, the hydrothermal resistance of two thiol/epoxy thermosetting polymers was comprehensively compared and evaluated. We anticipate that TMBPS/epoxy thermosetting polymer will achieve very excellent comprehensive performance, thereby possessing broad application prospects in the electronic packaging.

TMBPS can be obtained from 4,4′-sulfonyldiphenol (BPS) after a series of reactions (Fig. S1 in Supporting information). The detailed synthesis process is listed in Supporting information. In order to confirm the successful synthesis of TMBPS and its intermediates, the chemical structures were analyzed by ^{1}H NMR, ^{13}C NMR and FTIR (Figs. S2-S6 in Supporting information). In the ^{1}H NMR and FTIR spectra of TMBPS (Figs. S3 and S6), the signal peaks of -SH appeared at $\delta = 1.40$ ppm and 2565 cm^{-1}, which proved the successful synthesis of TMBPS. Detailed analysis of the process can be seen in Supporting information. In addition, the HPLC spectra of TMBPS and its intermediates are shown in Fig. S7 (Supporting information), and the sharp single peaks prove that TMBPS and its intermediates have high purity.

TMBPS and PETMP were respectively mixed with DGEBA according to the scheduled stoichiometric ratio (the molar ratio of thiol to epoxy group was 1:1). Then PN23 (1% of DGEBA mass) was added and mixed evenly. According to the different types of thiols, two kinds of thiol/epoxy thermosetting polymers were named as TMBPS/DGEBA and PETMP/DGEBA, respectively. After removing the bubbles in the vacuum oven, the mixture was added to the PTFE mold preheated at 70 °C. Then TMBPS/DGEBA was cured at 75 °C, 115 °C and 155 °C for 2 h respectively, and PETMP/DGEBA was cured at 90 °C, 110 °C and 125 °C for 2 h respectively. The curing temperature was determined by the curing kinetics of two thiol/epoxy systems, which will be described in detail below.

The molecular formulas of DGEBA, PN23, TMBPS and PETMP are depicted in Fig. S8 (Supporting information). The molecular structures of TMBPS and PETMP were simulated by Chem3D software. As shown in Fig. S9 (Supporting information), the distance between the two nearest thiol groups in the PETMP molecule is 5.461 Å, resulting in a significant steric hindrance which hinders the reaction of PETMP with the epoxy resin [33]. In contrast, the distance between the nearest thiol groups in TMBPS is greater and up to 6.998 Å, enabling a less-constrained and more-reactive interaction with the epoxy resin. In addition, we calculated the HOMO-LUMO energy gap of TMBPS and PETMP by frontier molecular orbital (FMO) analysis, as shown in Fig. S10 (Supporting information). The frontier orbital gap (HOMO-LUMO gap) is an important factor affecting the chemical reactivity and kinetic stability of molecules [34]. Molecule with low HOMO-LUMO gap has higher chemical reactivity. The HOMO-LUMO energy gap of TMBPS was 5.2044 eV, which was significantly lower than that of PETMP (6.4649 eV), indicating that the electrons of TMBPS are more easily excited from the HOMO level to the LUMO level [35], which proves that TMBPS has higher reactivity.

The curing mechanism of the thiol/epoxy system is shown in Fig. 1a, that is, the thiol group of TMBPS or PETMP reacts with the epoxy group of DGEBA to form a cross-linked network. The curing behaviors of the TMBPS/DGEBA and PETMP/DGEBA systems at different heating rates (5, 10, 15 and 20 K/min) were analyzed using non-isothermal differential scanning calorimetry (DSC). The corresponding DSC curves are shown in Figs. 1b and c, and the exothermic peak temperatures are listed in Table S1 (Supporting information). The curing conditions for TMBPS/DGEBA and PETMP/DGEBA were determined by linear fitting of the start temperature (T_s), peak temperature (T_p), and end temperature (T_e) with heating rate (β) and extrapolating to $\beta = 0$, as shown in Figs. 1d and e. The relevant data are shown in Table S2 (Supporting information). TMBPS/DGEBA has a lower initial curing temperature than PETMP/DGEBA, indicating that the TMBPS/DGEBA system has higher reactivity, which corresponds to the above simulation results of TMBPS and PETMP molecules. The two thiol/epoxy systems showed a single exothermic peak at different heating rates, indicating that there was no obvious side reaction between thiol and epoxy resin [36]. In addition, with the increase of heating rate, the exothermic peak gradually moved to the high temperature direction. This phenomenon was due to the reason that when the heating rate was higher, the curing time at a certain temperature was shorter, so the system had no time to cure and was accumulated to the next temperature to continue curing [37,38]. Compared with PETMP/DGEBA, the exothermic peak of TMBPS/DGEBA was wider, indicating that the heat release during curing was more uniform and the curing reaction was more sufficient. The four thiol groups of PETMP had the same activity, while there were two kinds of

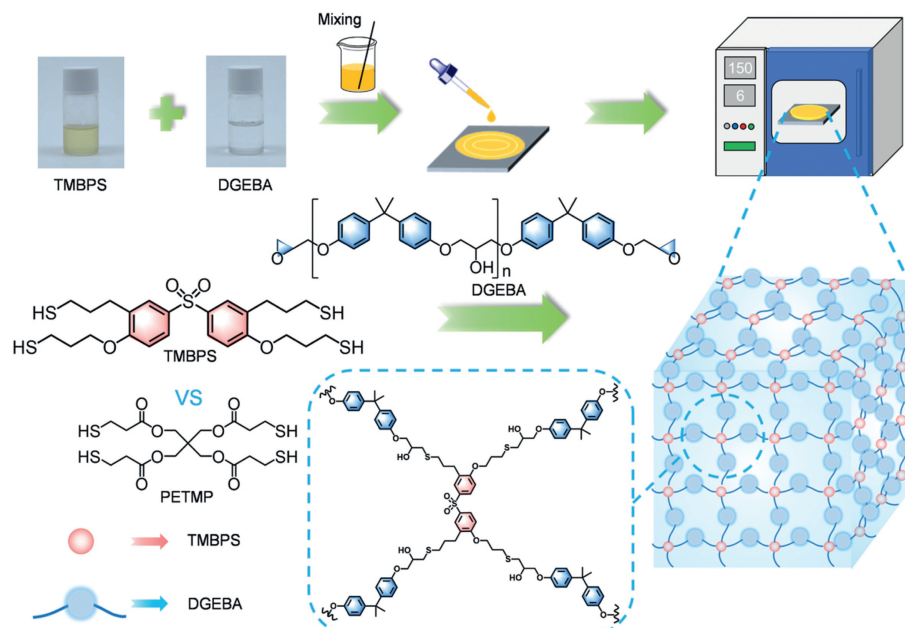

Scheme 1. Schematic illustration of the preparation process of thiol/epoxy thermosetting networks.

thiol groups with different reaction activities in TMBPS. The curing exothermic peak temperatures of the two thiol groups reacting with the epoxy resin are similar, so the overlap induced the total exothermic peak wider [39].

To compare the curing activity of two thiol/epoxy systems more accurately, the apparent activation energy (E_a) was calculated using the Kissinger method (Eq. S2 in Supporting information). Fig. 1f demonstrates that the near regression coefficients fitted from the Kissinger method were all greater than 0.996, indicating the accurate and reliable fitting results. The apparent activation energy of TMBPS/DGEBA was calculated to be 52.08 kJ/mol which was lower than that of PETMP/DGEBA reaching 66.89 kJ/mol, confirming that TMBPS/DGEBA was more reactive. The change in enthalpy (Table S1 in Supporting information) and conversion rate with temperature variation was determined by integrating the non-isothermal curves of the two thiol/epoxy systems (Figs. S11 and S12 in Supporting information). The conversion rate curves for the two systems at different heating rates were all S-shaped, indicating an autocatalytic effect [40]. To further investigate the curing behavior, the Kissinger-Akahira-Sunose (KAS) method (Eq. S3 in Supporting information) [41] was used to calculate the activation energy at different conversion rates. The straight lines fitted by the KAS method are shown in Figs. S13 and S14 (Supporting information), and the activation energy at different conversion rates is presented in Fig. 1g. The curing activation energy of PETMP/DGEBA decreased with the increase of conversion rate, confirming the autocatalytic behavior of the thiol/epoxy systems. However, the curing activation energy of TMBPS/DGEBA initially decreased and then increased with conversion rate. This trend is due to the increasing crosslinking density and viscosity as the reaction progresses, which enhances steric hindrance and reduces the likelihood of collisions between thiol and epoxy molecules [42]. Moreover, the average curing activation energies of TMBPS/DGEBA and PETMP/DGEBA were 53.70 kJ/mol and 62.17 kJ/mol, respectively, which closely matched the apparent activation energies calculated by the Kissinger method, further supporting the higher reactivity of TMBPS. The Kinssinger method is based on a simplified mathematical model and is suitable for simple reaction systems [43–45]. Therefore, the Kinssinger method is used to obtain a rough activation energy. The KAS method is a model-free isoconversional method [46,47], which provides more accurate kinetic parameters by considering the change of activation energy under different conversion rates. It is suitable for complex systems [48], and the calculated activation energy is also more accurate.

Additionally, the curing process of the TMBPS/DGEBA system was monitored using isothermal infrared spectroscopy at 80 °C to explore the changes in functional groups during curing. Fig. 1j displays the infrared spectrum of TMBPS/DGEBA over time. As the reaction proceeded, the thiol absorption peak (Fig. 1h) and the epoxy absorption peak (Fig. S15 in Supporting information) gradually decreased. After 100 min, the thiol characteristic peak had nearly disappeared, indicating the completion of the curing reaction. Furthermore, due to the ring-opening reaction between the epoxy group and the active hydrogen in the thiol group, new hydroxyl groups were formed, resulting in a gradual increase in the vibration peak at 3504 cm^{-1} (Fig. S16 in Supporting information). The conversion rate during curing was calculated based on changes in the thiol characteristic peak (Eq. S1 in Supporting information), as shown in Fig. 1i. With the progress of curing, the crosslinking density and steric hindrance in the system increased, leading to a final conversion rate of 86.7%.

During polymer processing, it is often necessary for the viscosity to be below 1 Pa s within the processing window. Rheological analysis was conducted to measure the viscosity of TMBPS, PETMP, and the two thiol/epoxy systems under various conditions. The viscosity changes of TMBPS and PETMP with shear rate and temperature are shown in Fig. 2a and Fig. S17 (Supporting information). TMBPS exhibited a significantly higher viscosity than that of PETMP due to the incorporation of a sulfone group and two rigid benzene rings in TMBPS. The viscosity of TMBPS decreased with the increase of shear rate, displaying the characteristic of a pseudoplastic fluid. Whereas the viscosity of PETMP remained constant across shear rates, identifying it to be a Newtonian fluid. Furthermore, due to the higher initial viscosity, the viscosity of TMBPS decreased sharply with temperature increasing. The complex viscosity-temperature curves of TMBPS/DGEBA and PETMP/DGEBA are shown in Fig. 2b. The viscosity of TMBPS/DGEBA was below 1 Pa s within the temperature range of 61.8–141.3 °C, yielding a processing window of 79.5 °C, while PETMP/DGEBA ex-

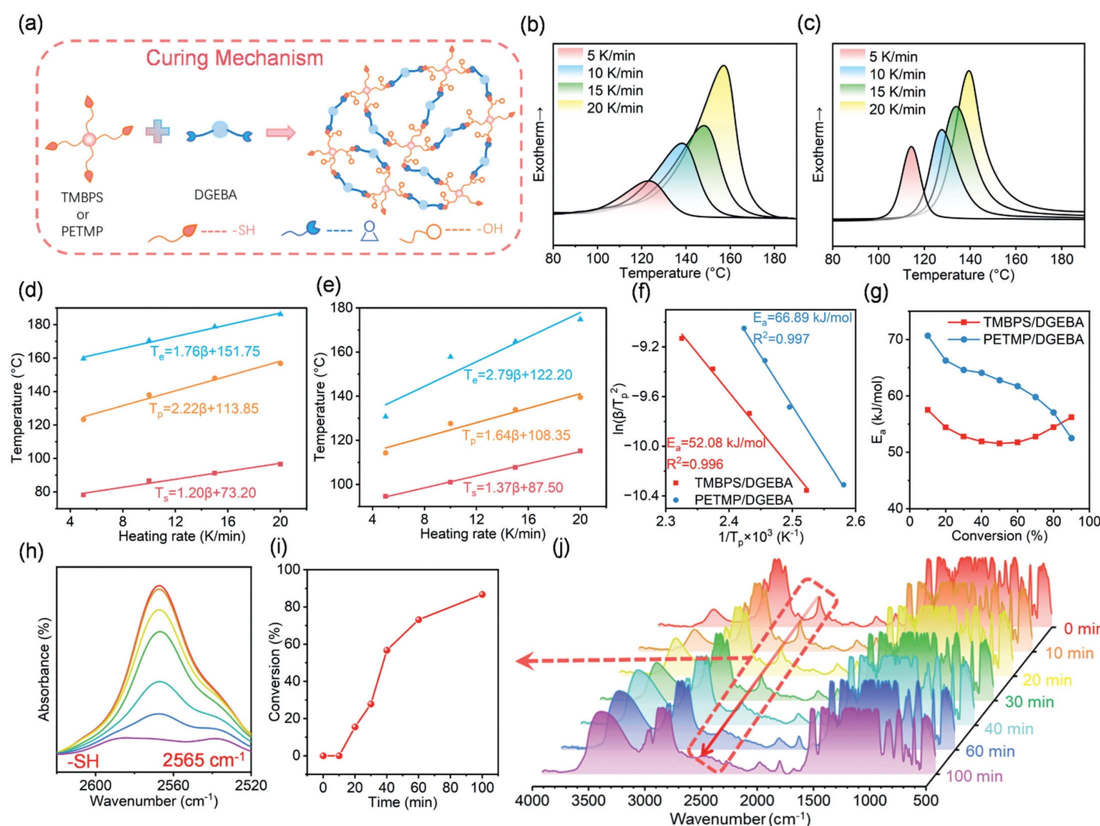

Fig. 1. The curing process of TMBPS/DGEBA and PETMP/DGEBA. (a) Curing mechanism of thiol/epoxy systems. DSC curves of (b) TMBPS/DGEBA and (c) PETMP/DGEBA. Extrapolate curves of curing system of (d) TMBPS/DGEBA and (e) PETMP/DGEBA. (f) The linear fitting curve obtained by Kissinger method. (g) Changes of curing activation energy with conversion rate. (h) Infrared characteristic peaks of thiol groups at different curing stages, (i) curve of thiol conversion rate, (j) FTIR spectra at different curing stages of TMBPS/DGEBA.

hibited a processing window of 97.7 °C, indicating good processing performance for both thiol/epoxy systems.

The thermal stability of the two thiol/epoxy thermosetting polymers under a nitrogen atmosphere was evaluated using thermogravimetric analysis (TGA). As depicted in Figs. 2c and d, with relevant data provided in Table S3 (Supporting information), the initial decomposition temperature ($T_{d5\%}$) and the temperature at 50% weight loss ($T_{d50\%}$) for TMBPS/DGEBA were respectively 318.0 °C and 376.0 °C which were both higher than those for PETMP/DGEBA ($T_{d5\%}=315.4$ °C, $T_{d50\%}=349.9$ °C. Additionally, the residual carbon rate of TMBPS/DGEBA at 800 °C was 16.3% which was 2.8 times higher than that of PETMP/DGEBA. To further compare the thermal stability of two polymers, the statistical heat resistance index (T_s) [49] was calculated by Eq. S4 (Supporting information). The T_s of TMBPS/DGEBA was 167.3 which was higher than that of PETMP/DGEBA (T_s=160.9), indicating its superior thermal stability that attributed to the advantageous structure of TMBPS.

The chemical stability of thermosetting polymers affects their durability and potential applications. Therefore, we investigated the stability of the two thiol/epoxy thermosetting polymers in different chemical environments. The polymers were immersed in NaCl (10 wt%), NaOH (10 wt%), HCl (10 wt%), and anhydrous ethanol to observe their changes for 30 days at 25 °C and 48 h at 80 °C (Fig. S18 in Supporting information and Fig. 2g). The change in residual mass was calculated by Eq. S5 (Supporting information), as shown in Figs. 2e and f. At 25 °C, the mass of TMBPS/DGEBA remained nearly unchanged in all the testing environments, while PETMP/DGEBA lost approximately 25% of its mass in NaOH (10 wt%). Higher temperatures accelerated the mass loss in these polymers. At 80 °C, PETMP/DGEBA completely degraded in NaOH (10 wt%) and exhibited structural changes in HCl (10 wt%), indicating the structural damage and mass loss, whereas TMBPS/DGEBA remained stable in these severe environments. These results indicated that TMBPS/DGEBA exhibited better stability than PETMP/DGEBA under acidic and alkaline conditions. Due to the existence of a large number of ester bonds in the structure of PETMP/DGEBA, it is easy to hydrolyze under acidic and alkaline conditions [50], resulting in the fracture of the molecular structure of PETMP, which causes the PETMP/DGEBA crosslinking network to decompose. The resulting voids allow more solvent molecules to penetrate, thereby accelerating the decomposition of the crosslinking network. The ester-free structure of TMBPS endows it with excellent chemical resistance. TMBPS molecules will not decompose under acidic and alkaline conditions and the TMBPS/DGEBA crosslinking network will prevent more solvent molecules from penetrating after accommodating sufficient solvent molecules.

The storage modulus and glass transition temperature (T_g) of the two thiol/epoxy thermosetting polymers were measured by dynamic thermomechanical analysis (DMA), with the results presented in Figs. 2h and i, and corresponding data listed in Table S4 (Supporting information). The storage modulus of TMBPS/DGEBA was consistently higher than that of PETMP/DGEBA during the entire experimental temperature range, particularly between 40 °C and 70 °C. The T_g is the highest temperature at which thermosetting materials can be effectively used, corresponding to the main peak of tanδ in Fig. 2i. The T_g of TMBPS/DGEBA was 74.2 °C which was 11.8 °C higher than that of PETMP/DGEBA. This difference was attributed to the molecular rigidity and crosslinking density of the polymers. According to the theory of rubber elasticity,

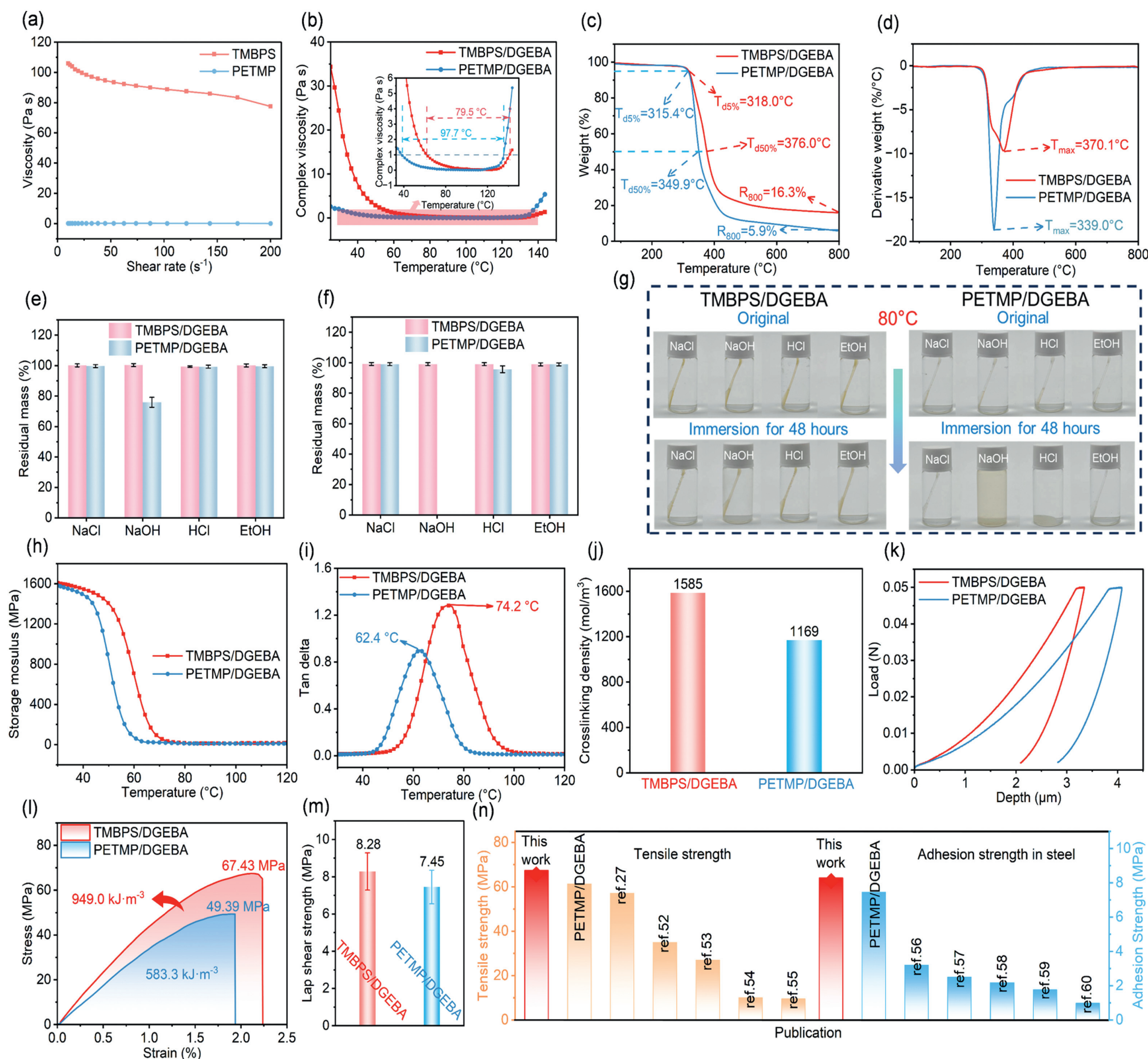

Fig. 2. The machinability (a, b), stability (c-g) and mechanical properties (h-n) of TMBPS/DGEBA and PETMP/DGEBA. (a) The viscosity-shear rate curves at 25 °C of TMBPS and PETMP. (b) Viscosity-temperature curve at 10 s^{-1} shear rate of TMBPS/DGEBA and PETMP/DGEBA. (c) TGA curve and (d) DTG curve in N_2. Residual mass histograms of samples immersed in different solutions at (e) 25 °C and (f) 80 °C. (g) Digital photographs of samples immersed in different solutions at 80 °C. (h) Storage elastic curve, (i) tanδ curve, (j) crosslinking density, (k) load-depth curve, (l) stress-strain curve, (m) adhesion strength in steel of TMBPS/DGEBA and PETMP/DGEBA. (n) The tensile strength and adhesion strength of TMBPS/DGEBA and PETMP/DGEBA were compared with other materials reported in the literature.

the crosslinking density (V_e) of the two thiol/epoxy thermosetting polymers was calculated by Eq. S6 (Supporting information) [51]. The calculated V_e for TMBPS/DGEBA was 1585 mol/m³ which was higher than that of PETMP/DGEBA (V_e = 1169 mol/m³), as shown in Fig. 2j, likely due to the higher reactivity of the thiol group in TMBPS, which allows for more complete reaction with the epoxy resin.

The mechanical properties of the thiol/epoxy thermosetting polymers were further evaluated by nanoindentation experiments, with the load-depth curves shown in Fig. 2k. Under identical external forces, the indentation depth of TMBPS/DGEBA was smaller than that of PETMP/DGEBA. Additionally, the hardness and Young's modulus of the two polymers were calculated by Eqs. S7 and S8 (Supporting information). TMBPS/DGEBA exhibited a hardness of 0.23 GPa and a Young's modulus of 3.99 GPa which were 1.6 times and 1.2 times greater than those of PETMP/DGEBA, respectively. Furthermore, the mechanical properties were assessed by measuring the tensile strength and adhesion strength, as shown in Figs. 2l and m. The tensile strength and adhesion strength of TMBPS/DGEBA were respectively to be 67.43 MPa and 8.28 MPa which were both higher than those of PETMP/DGEBA (49.39 MPa and 7.45 MPa, respectively). In addition, although both of them exhibited brittle fracture (Fig. S19 in Supporting information), TMBPS/DGEBA exhibited more excellent toughness than PETMP/DGEBA. A comparison of the tensile and adhesion strengths of TMBPS/DGEBA and PETMP/DGEBA with literature data (Fig. 2n) [27,52–60] indicates that TMBPS/DGEBA exhibits excellent tensile and adhesion properties, which can be attributed to the polymer's crosslinking density and stiffness [61].

Prolonged ultraviolet radiation can cause the breakage of polymer molecular chains or covalent bonds, resulting in the destruction of the structure and properties of the material [62].

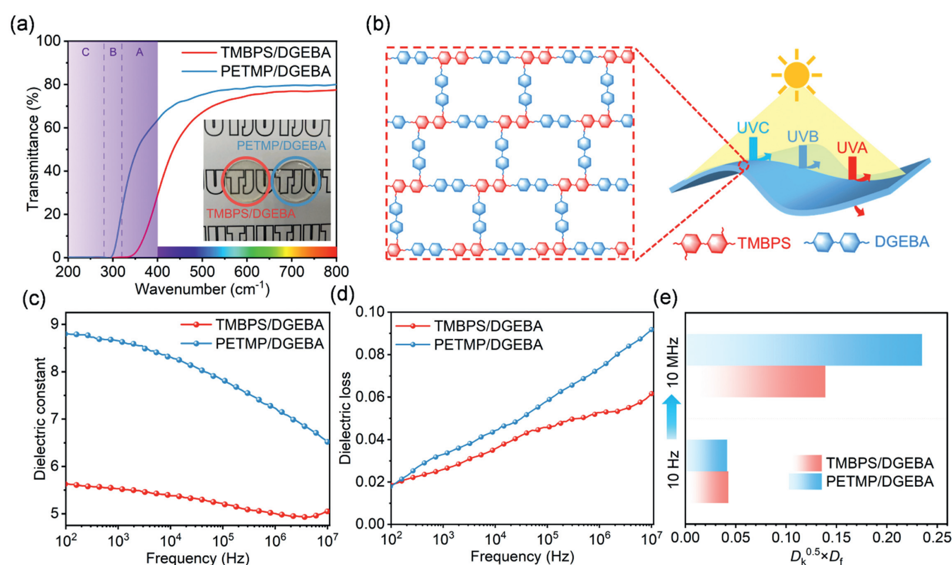

Fig. 3. UV-shielding and dielectric properties of TMBPS/DGEBA and PETMP/DGEBA. (a) UV–vis spectrum. (b) Schematic diagram of UV absorption principle of TMBPS/DGEBA. (c) Dielectric constant, (d) dielectric loss and (e) the value of $D_k^{0.5} \times D_f$ at different frequencies.

The ultraviolet transmittance of the thiol/epoxy systems were tested by an ultraviolet-visible-near-infrared spectrophotometer, with results presented in Fig. 3a. Compared to PETMP/DGEBA, TMBPS/DGEBA exhibited a significantly greater UV-blocking ability. Specifically, TMBPS/DGEBA effectively blocked all UVB and UVC rays, with a transmission rate of <27% in the UVA region. Fig. 3b illustrates the UV absorption mechanism of TMBPS/DGEBA, which is attributed to its high benzene ring content [63]. The stable conjugated system of benzene ring could facilitate the Π electron transitions that absorbing UV light.

The dielectric properties of materials are critical for their safety and effectiveness in specific electrical applications. To analyze the dielectric properties of thiol/epoxy thermosetting polymers, these properties were evaluated across a wide frequency range. Figs. 3c and d show the variation of dielectric constant and dielectric loss with frequency. Over the frequency range of 10^2–10^7 Hz, TMBPS/DGEBA exhibited a lower dielectric constant than that of PETMP/DGEBA. This difference can be attributed to the large number of polar ester bonds in PETMP/DGEBA, which contribute to a higher dipole moment and dielectric constant [64,65]. Conversely, the introduction of rigid structures in the TMBPS restricts dipole rotation, resulting in a lower dielectric constant. The variation in dielectric loss with frequency is depicted in Fig. 3d. At the low electric field frequencies, the dipole moment changes synchronously with the external electric field, and the dielectric loss is primarily due to the conductance loss of free ions. As the frequency increases, the dipole motion lags behind the external field changes, leading to the dielectric loss that mainly due to dipole relaxation [66]. Notably, TMBPS/DGEBA exhibited a lower dielectric loss than that of PETMP/DGEBA across the tested frequency range, likely due to the reduced molecular chain mobility in the TMBPS/DGEBA system. Theoretically, signal propagation loss is determined by the product of the square root of the dielectric constant (D_k) and dielectric loss factor (D_f). A higher product value induces signal propagation loss. As shown in Fig. 3e and Table S5 (Supporting information), although the values of both thermosetting polymers were similar at 100 Hz, the gap widened significantly at higher frequencies. At 10 MHz, the product value for PETMP/DGEBA was approximately 1.7 times of TMBPS/DGEBA, suggesting that TMBPS/DGEBA offered better signal propagation efficiency. Additionally, dielectric strength tests in an alternating electric field (Fig. S20 in Supporting information) revealed that TMBPS/DGEBA has a dielectric strength of 23.1 kV/mm which was 3.6 kV/mm higher than that of PETMP/DGEBA, indicating superior resistance of TMBPS/DGEBA to voltage breakdown.

Thermosetting polymers are often exposed to the hot and humid environments which can lead to internal stress and degradation after water absorption, ultimately reducing their performances. The water absorption process primarily involves surface adsorption and internal diffusion [67]. To evaluate the water adsorption capacities on the surface of two thiol/epoxy thermosetting polymers, we measured their static water contact angles, as shown in Fig. 4a. Compared to PETMP/DGEBA, TMBPS/DGEBA displayed a better hydrophobicity. We further assessed the water resistance of these polymers at 25 °C and 80 °C, calculating the change in water absorption by Eq. S9 (Supporting information). The results, presented in Figs. 4b and c, show that TMBPS/DGEBA consistently exhibited lower water absorption than PETMP/DGEBA. After soaking at 25 °C for 6 days and at 80 °C for 12 h, the water absorption rate of PETMP/DGEBA was approximately 2.6 times of TMBPS/DGEBA. This difference is attributed to the higher hydrophobic benzene ring content in TMBPS/DGEBA. The large volume of hydrophobic benzene rings can block the penetration of water into the network, thus significantly reducing the water absorption of TMBPS/DGEBA [68].

We also evaluated the changes in tensile strength and adhesion strength of the two thiol/epoxy thermosetting polymers after exposure to high-temperature and high-humidity conditions (85 °C and 85% RH) over different time intervals. Figs. 4d and e show the stress-strain curves after various test durations, while Fig. 4f presents the corresponding changes in tensile strength and elongation at break. The high ester bond content in PETMP makes it prone to be hydrolyzed under these conditions. After 500 h of testing, the tensile strength of PETMP/DGEBA decreased from 49.39 MPa to 3.17 MPa, and the elongation at break increased from 1.33% to 98.76%. By 750 h, PETMP/DGEBA had lost all tensile strength. In contrast, TMBPS/DGEBA exhibited more π-π stacking, higher crosslinking density, and an ester-free structure, leading to a greater stability. Its tensile strength remained stable at 66.89 ± 6.44 MPa, and its elongation at break remained steady at 2.89% ± 0.65%. Notably, the tensile strength of TMBPS/DGEBA in-

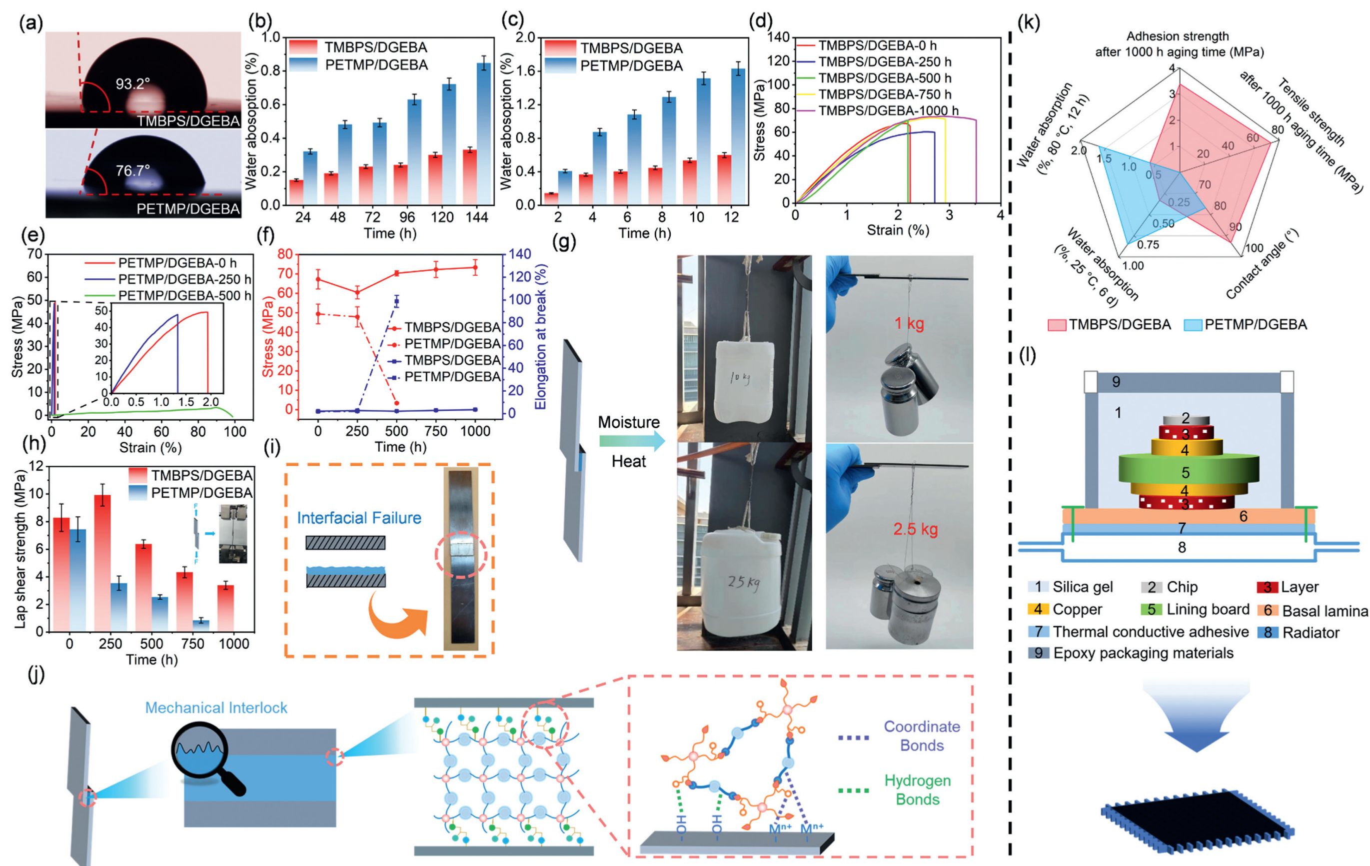

Fig. 4. The hygrothermal resistance of TMBPS/DGEBA and PETMP/DGEBA. (a) Static contact angle. (b) Water absorption at 25 °C and (c) 80 °C. Stress-strain curves of (d) TMBPS/DGEBA and (e) PETMP/DGEBA after different hygrothermal aging test time. (f) The change of tensile strength and elongation at break with the experimental time. (g) The steel plate bonded by TMBPS/DGEBA after 1000 h hygrothermal aging test can load 2.5 kg weight horizontally and 25 kg weight vertically. (h) The change of lap shear strength of steel with experimental time. (i) The adhesion failure mode of TMBPS/DGEBA after 1000 h hygrothermal aging test. (j) The schematic diagram of adhesion principle. (k) Comparison of hygrothermal resistance of two thiol/epoxy thermosetting polymers. (l) TMBPS/DGEBA has potential electronic packaging applications.

creased slightly over time due to the enhanced curing degree and crosslinking density at elevated temperatures.

Fig. 4h illustrates the variation in lap shear strength of the two thiol/epoxy thermosetting polymers on steel over time. Adhesion strength is primarily determined by the combined effects of adhesion and cohesion [69]. Cohesion is dependent on the forces between polymer molecular chains, while the adhesion in the two materials is mainly relied on the hydrogen bonds and coordinate bonds formed between exposed hydroxyl groups on the molecular chain and the substrate, as well as the close mechanical interlock between the material and the substrate surface (Fig. 4j) [57]. The hydroxyl groups on the molecular chain come from the hydroxyl groups produced by the ring-opening reaction of thiol with epoxy resin and the hydroxyl groups of epoxy resin itself. High-temperature and high-humidity conditions caused significant changes in the adhesion strength of both polymers. After 250 h of aging, the adhesion strength of TMBPS/DGEBA to steel increased slightly due to post-curing, which enhanced crosslinking density and cohesion. However, as aging continued, the adhesion strength gradually decreased, reaching 3.39 MPa at 1000 h, which was about 41.1% of its initial value. After testing the lap shear strength after 1000 h of aging, we noticed that TMBPS/DGEBA was distributed on one side of the substrate, as shown in Fig. 4i, which proved that it was an interfacial failure mode between it and the steel substrate. This failure mode is attributed to the breakage of hydrogen bonds and coordinate bonds in high temperature environment and the weakening of mechanical interlocking caused by molecular chain motion. Despite this, after 1000 h of testing, the TMBPS/DGEBA-coated steel plate could support a horizontal load of 2.5 kg and a vertical load of 25 kg without breaking (Fig. 4g). In contrast, the adhesion strength of PETMP/DGEBA decreased steadily over time. In addition to the breaking of hydrogen bonds and coordinate bonds and the weakening of mechanical interlocking, the PETMP/DGEBA molecular chains containing a large number of ester bonds could undergo hydrolysis under high-temperature and high-humidity conditions, leading to a loss of cohesion. The combined effects of these factors caused the adhesion strength of PETMP/DGEBA to completely disappear after 1000 h.

Therefore, TMBPS/DGEBA exhibits better hygrothermal resistance than PETMP/DGEBA (Fig. 4k). As the protective shell of the chip (Fig. 4l), the performance of epoxy packaging material is very important, and the TMBPS/DGEBA with excellent hygrothermal resistance can effectively protect the electronic device from damage, so it has potential applications in the field of electronic packaging.

In summary, the bisphenol S-type tetrafunctional thiol compound TMBPS was successfully synthesized from bisphenol S in this study. TMBPS exhibited many advantages over the commercial thiol PETMP due to its unique structural features, including rigid benzene rings, a polar sulfone group, and the ester-free structure. After reacting with DGEBA, the TMBPS/DGEBA system displayed a T_g of 74.2 °C which was 11.8 °C higher than that of the PETMP/DGEBA system, significantly enhancing the heat resistance. Additionally, the hardness and tensile strength of TMBPS/DGEBA were 0.23 GPa and 67.43 MPa, respectively, representing increases of 61.4% and 36.5% over those of PETMP/DGEBA. Compared to PETMP/DGEBA, the TMBPS/DGEBA system also showed significantly

improved chemical resistance, water resistance, dielectric properties, and UV-shielding performance. Notably, after 1000 h of high-temperature and high-humidity aging, the tensile strength and adhesion strength of TMBPS-cured products were 73.33 MPa and 3.39 MPa, while the PETMP-cured product completely lost its tensile and adhesion strengths. This research paves the way for the synthesis of thermosetting polymers that can be cured at low temperatures while exhibiting excellent overall properties, thereby possessing broad application prospects in the electronic packaging.

Declaration of competing interest

The authors declare that they have no known competing financial interests or personal relationships that could have appeared to influence the work reported in this paper.

CRediT authorship contribution statement

Chunshi He: Writing – original draft, Software, Methodology, Investigation, Formal analysis, Data curation, Conceptualization. **Linqing Li:** Validation, Formal analysis. **Yuanrong Sun:** Software, Data curation. **Xuefang Wang:** Methodology, Formal analysis. **Jie Ren:** Visualization, Validation. **Jianbo Li:** Writing – review & editing, Supervision, Resources, Funding acquisition, Conceptualization.

Acknowledgments

The authors gratefully acknowledge the support of the Science and Technology Commission of Shanghai Municipality (STCSM, No. 20dz1203600) and the Experimental Center of Materials Science and Engineering in Tongji University.

Supplementary materials

Supplementary material associated with this article can be found, in the online version, at doi:10.1016/j.cclet.2025.110905.

References

[1] S. Kumar, S.K. Samal, S. Mohanty, S.K. Nayak, Polym. Plast. Technol. Eng. 57 (2018) 133–155.
[2] M.M.A. Baig, M.A. Samad, Polymers 13 (2021) 179.
[3] Z. Yu, S. Ma, Z. Tang, et al., Green Chem. 23 (2021) 6566–6575.
[4] S. Zhou, Z. Chen, R. Tusiime, et al., Compos. Commun. 13 (2019) 80–84.
[5] X. Wang, B. Ma, K. Wei, W. Zhang, Constr. Build. Mater. 312 (2021) 125392.
[6] Z. Chen, X. Liu, H. Chen, et al., Chin. Chem. Lett. 35 (2024) 109194.
[7] X.M. Ding, L. Chen, X. Luo, et al., Chin. Chem. Lett. 33 (2022) 3245–3248.
[8] Q. Fan, J. Li, Q. Cao, et al., Compos. Commun. 51 (2024) 102068.
[9] J.M. Sousa, J.R. Correia, S. Cabral-Fonseca, Constr. Build. Mater. 161 (2018) 618–633.
[10] A. Credo, M. Villani, M. Popescu, N. Riviere, IEEE Trans. Ind. Appl. 57 (2021) 6440–6452.
[11] J. Hou, J. Sun, Q. Fang, Polym. Chem. 14 (2023) 3203–3212.
[12] S. Budhe, M.D. Banea, S. de Barros, Appl. Adhes. Sci. 6 (2018) 3.
[13] Y. Qi, Z. Weng, K. Zhang, et al., Chem. Eng. J. 387 (2020) 124115.
[14] Y. Li, J. Li, W. Zhang, et al., Polymer 297 (2024) 126836.
[15] Z. Miao, D. Yan, X. Wang, et al., Chin. Chem. Lett. 33 (2022) 4026–4032.
[16] W. Zhang, Z. Yan, L. Chen, Y. Xiao, Chin. Chem. Lett. 35 (2024) 109582.
[17] M.Z. Rong, M.Q. Zhang, W. Zhang, Adv. Compos. Lett. 16 (2007) 167–172.
[18] S.J. Park, F.L. Jin, Polym. Degrad. Stab. 86 (2004) 515–520.
[19] B. Liu, Q. Cao, J. Li, et al., Chin. Chem. Lett. 34 (2023) 108465.
[20] D. Balgude, A. Sabnis, S.K. Ghosh, Prog. Org. Coat. 104 (2017) 250–262.
[21] S.M. Hong, O.Y. Kim, S.H. Hwang, RSC Adv. 11 (2021) 34263–34268.
[22] A. Gomez-Lopez, B. Grignard, I. Calvo, et al., ACS Appl. Polym. Mater. 4 (2022) 8786–8794.
[23] S.M. Hong, S.H. Hwang, Polym. Test. 110 (2022) 107593.
[24] Y.H. Kim, J.J. Baek, K.C. Chang, et al., Polymers 15 (2023) 2947.
[25] Y. Wang, L. Tang, Y. Li, Q. Li, J. Appl. Polym. Sci. 139 (2022) 51548.
[26] Y. Lu, Y. Wang, S. Chen, et al., Prog. Org. Coat. 139 (2020) 105436.
[27] Y. Zhai, D. Zhang, L. Gao, Eur. Polym. J. 206 (2024) 112767.
[28] D. Kim, C. Yu, Y. Kwon, et al., ACS Appl. Polym. Mater. 5 (2023) 9046–9055.
[29] Y. Ke, X. Yang, Q. Chen, et al., ACS Appl. Polym. Mater. 3 (2021) 3082–3092.
[30] D. Guzmán, A. Serra, X. Ramis, et al., React. Funct. Polym. 136 (2019) 153–166.
[31] D. Guzmán, B. Mateu, X. Fernández-Francos, et al., Polym. Int. 66 (2017) 1697–1707.
[32] S. Reinelt, M. Tabatabai, U.K. Fischer, et al., Beilstein J. Org. Chem. 10 (2014) 1733–1740.
[33] T. Liu, L. Zhang, R. Chen, et al., Ind. Eng. Chem. Res. 56 (2017) 7708–7719.
[34] N.M. Sabry, R. Badry, F.K. Abdel-Gawad, et al., Sci. Rep. 14 (2024) 22801.
[35] M. Miar, A. Shiroudi, K. Pourshamsian, et al., J. Chem. Res. 45 (2020) 147–158.
[36] W. Hao, J. Hu, L. Chen, et al., Polym. Test. 30 (2011) 349–355.
[37] J.L. Huang, H.L. Ding, X. Wang, et al., Chem. Eng. J. 450 (2022) 137906.
[38] W. Mao, S. Li, X. Yang, et al., J. Therm. Anal. Calorim. 130 (2017) 2113–2121.
[39] Y. Qi, Z. Weng, Y. Kou, et al., Compos. B: Eng. 214 (2021) 108749.
[40] J.Y. Lee, M.J. Shim, S.W. Kim, Mater. Chem. Phys. 48 (1997) 36–40.
[41] Q. Bi, L. Hao, Q. Zhang, et al., Thermochim. Acta 678 (2019) 178302.
[42] X. Liu, H. Wang, B. Zeng, et al., Compos. B: Eng. 273 (2024) 111260.
[43] S. Vyazovkin, A.K. Burnham, J.M. Criado, et al., Thermochim. Acta 520 (2011) 1–19.
[44] X. Zhang, Eng. Sci. 14 (2021) 1–13.
[45] S. Vyazovkin, Molecules 25 (2020) 2813.
[46] E. Tarani, K. Chrissafis, Thermochim. Acta 733 (2024) 179690.
[47] G. Mashouf Roudsari, A.K. Mohanty, M. Misra, ACS Sustainable Chem. Eng. 2 (2014) 2111–2116.
[48] M.J. Starink, Thermochim. Acta 404 (2003) 163–176.
[49] S. Ma, X. Liu, L. Fan, et al., ChemSusChem 7 (2014) 555–562.
[50] Z. Khan, F. Javed, Z. Shamair, et al., Ind. Eng. Chem. Res. 103 (2021) 80–101.
[51] H. Nabipour, X. Wang, L. Song, Y. Hu, Green Chem. 23 (2021) 501–510.
[52] B. Zhang, X. Yang, X. Lin, et al., ACS Sustainable Chem. Eng. 11 (2023) 6100–6113.
[53] R. Song, X. Wang, M. Johnson, et al., Adv. Funct. Mater. 34 (2024) 2313322.
[54] T. Türel, B. Eling, A.M. Cristadoro, et al., ACS Appl. Mater. Interfaces 16 (2024) 6414–6423.
[55] Y. Zhou, J. Luo, Q. Jing, et al., Adv. Funct. Mater. 34 (2024) 2406557.
[56] H. Ju, Z. Yin, Z. Demchuk, et al., Adv. Funct. Mater. 34 (2024) 2402165.
[57] Q. Zhu, R. Li, Y. Yan, et al., Adv. Funct. Mater. 34 (2024) 2402734.
[58] Q. Du, B. Hu, Q. Shen, et al., Chem. Eng. J. 482 (2024) 148828.
[59] K. Jiang, X. Dong, Y. Chen, et al., Adv. Funct. Mater. 34 (2024) 2403490.
[60] W. Cao, X. Duan, Z. Zhang, et al., Chem. Eng. J. 482 (2024) 148199.
[61] T.Y. Gao, F.D. Wang, Y. Xu, et al., Chem. Eng. J. 428 (2022) 131173.
[62] M. Diepens, P. Gijsman, Polym. Degrad. Stab. 92 (2007) 397–406.
[63] Y. Zhang, J. Jing, T. Liu, et al., Chem. Eng. J. 411 (2021) 128493.
[64] Q. Luo, H. Shen, G. Zhou, X. Xu, Carbohydr. Polym. 303 (2023) 120449.
[65] A. Khouaja, A. Koubaa, H.Ben Daly, Ind. Crops Prod. 214 (2024) 118493.
[66] M. Qin, L. Zhang, H. Wu, Adv. Sci. 9 (2022) 2105553.
[67] A. Xing, F. Bao, J. Fu, et al., Polym. Test. 71 (2018) 38–48.
[68] J. Liu, X. Liu, X. Cui, et al., Polym. Chem. 14 (2023) 1665–1679.
[69] A. Bal-Ozturk, B. Cecen, M. Avci-Adali, et al., Nano Today 36 (2021) 101049.